SbcB facilitates natural transformation in *Vibrio cholerae* in an exonuclease-independent manner

Triana N. Dalia[1] and Ankur B. Dalia[1,*]

[1]Department of Biology, Indiana University, Bloomington, IN 47405.
*Correspondence to: ankdalia@iu.edu

ABTRACT
Natural transformation (NT) is a conserved mechanism of horizontal gene transfer in bacterial species. During this process, DNA is taken up into the cytoplasm where it can be integrated into the host genome by homologous recombination. We have previously shown that some cytoplasmic exonucleases inhibit NT by degrading ingested DNA prior to its successful recombination. However, one exonuclease, SbcB, counterintuitively promotes NT in *Vibrio cholerae*. Here, through a systematic analysis of the distinct steps of NT, we show that SbcB acts downstream of DNA uptake into the cytoplasm, but upstream of recombinational branch migration. Through mutational analysis, we show that SbcB promotes NT in a manner that does not rely on its exonuclease activity. Finally, we provide genetic evidence that SbcB directly interacts with the primary bacterial recombinase, RecA. Together, these data advance our molecular understanding of horizontal gene transfer in *V. cholerae*, and reveal that SbcB promotes homologous recombination during NT in a manner that does not rely on its canonical exonuclease activity.

IMPORTANCE
Horizontal gene transfer by natural transformation contributes to the spread of antibiotic resistance and virulence factors in bacterial species. Here, we study how one protein, SbcB, helps facilitate this process in the facultative bacterial pathogen *Vibrio cholerae*. SbcB is a well-known for its exonuclease activity (*i.e.*, the ability to degrade the ends of linear DNA). Through this study we uncover that while SbcB is important for natural transformation, it does not facilitate this process using its exonuclease activity. Thus, this work helps further our understanding of the molecular events required for this conserved evolutionary process, and uncovers a function for SbcB beyond its canonical exonuclease activity.

INTRODUCTION
Cells can acquire novel traits through horizontal gene transfer by natural transformation. During this process, cells take up free double-stranded DNA (dsDNA) from the environment. In Gram-negative bacteria, dsDNA is first taken up across the outer membrane via the combined action of dynamic DNA-binding type IV pili (1, 2) and the periplasmic DNA-binding molecular ratchet ComEA (3, 4). Then, a single strand of this DNA is translocated across the inner membrane by ComEC and ComF(C). Once this single-stranded DNA (ssDNA) is translocated into the cytoplasm, it can interact with proteins that help facilitate its integration into the host genome. This includes DprA, which protects ingested DNA and helps recruit RecA to initiate homologous recombination (5).

Because the tDNA that is imported into the cytoplasm is ssDNA, it is potentially sensitive to the action of ssDNA exonucleases that may act to degrade this DNA before it can be integrated into the genome. Indeed, we have previously found that deletion of the ssDNA exonucleases *recJ*

and *exoVII* enhances NT in *V. cholerae* (6). In particular, Δ*recJ* Δ*exoVII* mutants can be transformed at high rates with tDNA containing short arms of homology (6), which is consistent with these proteins normally degrading the ends of ssDNA tDNA in the cytoplasm to inhibit NT.

Contrary to this negative effect of the RecJ and ExoVII ssDNA exonucleases on NT, our prior results suggest that one ssDNA exonuclease, SbcB, is required for optimal NT in *V. cholerae* (6). SbcB is one of the most well-studied bacterial exonucleases, primarily having been characterized in the model microbe *Escherichia coli*. It was originally identified biochemically and called Exonuclease I or ExoI (7), and subsequent genetic analysis uncovered the gene responsible and referred to it as SbcB (8) and XonA (9). In this study, we sought to determine how SbcB counterintuitively promotes NT in *V. cholerae*.

RESULTS

SbcB is required for optimal NT

The genes required for NT in *V. cholerae* are tightly regulated and induced via two distinct regulatory inputs: chitin oligosaccharides and quorum sensing (10, 11). Our prior experiments assessed the impact of *sbcB* on NT in a strain background that is dependent on both of these regulatory inputs. Thus, one possibility is that SbcB is important for regulating the expression of genes required for NT. Regulatory control of NT can be bypassed by ectopically expressing the master regulator of competence TfoX (10) and by constitutively activating quorum sensing via deletion of LuxO (1, 11, 12). So to test this hypothesis, we assessed the impact of *sbcB* on NT in a background where *tfoX* is ectopically expressed (P_{tac}-*tfoX*) and *luxO* is deleted. In this genetic background, we found that Δ*sbcB* exhibited a ~1.5-log decrease in NT (**Fig. 1**), which phenocopies what was previously observed when cells relied on natural induction via chitin and quorum sensing (6). This indicates that SbcB acts downstream of the regulatory steps that lead the expression of genes required for NT. All strains used throughout the remainder of the study contained P_{tac}-*tfoX* and Δ*luxO* mutations, which allowed us to bypass the need for chitin induction to study the effect of SbcB on NT.

SbcB does not facilitate the uptake of tDNA during NT

Next, we sought to identify the step of NT that is affected by SbcB. The first step of NT is the uptake of DNA from the environment, which requires the combined activities of dynamic DNA-binding competence type IV pili (T4P) to initiate the translocation of DNA across the outer membrane and a DNA-binding periplasmic molecular ratchet called ComEA. ComEA is a periplasmic dsDNA-binding protein, and it dynamically relocalizes upon DNA uptake, which can be monitored via functional fluorescent fusions like ComEA-mCherry (3, 4). The localization of ComEA-mCherry shifts from diffuse within the periplasm in the absence of tDNA uptake, to the formation of fluorescent foci when dsDNA is taken up into the periplasm (**Fig. 2A**). Thus, tracking the formation of ComEA-mCherry foci can allow for quantification of DNA uptake across the outer membrane. We assessed the formation of ComEA-mCherry foci after cells were incubated with tDNA for 30 mins (**Fig. 2A**). In the parent strain, almost all cells exhibited 1 or more ComEA-mCherry focus after this 30 min incubation (**Fig. 2B**). Consistent with tDNA uptake requiring T4P, mutating the critical T4P component PilQ (13, 14) prevents the formation of ComEA-mCherry foci (**Fig. 2B**). When we tested the *sbcB* mutant, we found that this strain could take up DNA into the periplasm in a manner that was indistinguishable from the parent (**Fig. 2B**; compare 30 min timepoints).

Following the uptake of dsDNA into the periplasm, a single strand of this tDNA is translocated across the inner membrane into the cytoplasm via the integral membrane protein ComEC (15, 16). And it is hypothesized that the strand of DNA that is not translocated into the cytoplasm is

102 degraded. The molecular mechanism underlying the translocation of this single-stranded tDNA
103 across the inner membrane remains very poorly understood. However, single cell tracking of the
104 spatiotemporal dynamics of tDNA integration are consistent with the recombination of ssDNA
105 (17). Thus, we hypothesized that SbcB could be facilitating NT by promoting the degradation of
106 one strand of tDNA to help translocate ssDNA into the cytoplasm. So, we next sought to test
107 whether SbcB affects the translocation of tDNA into the cytoplasm.
108
109 In *V. cholerae*, the translocation of DNA across the outer and inner membranes is temporally
110 uncoupled (18). Consistent with this, we find that the number of ComEA-mCherry foci in the
111 Δ*comEC* strain following a 30 min incubation with tDNA is indistinguishable from the parent
112 (**Fig. 2B**), indicating that the Δ*comEC* mutant still exhibits normal tDNA uptake into the
113 periplasm. Because uptake across the two membranes is uncoupled, we hypothesized that the
114 translocation of tDNA from the periplasm to the cytoplasm could be tracked indirectly using the
115 same ComEA-mCherry reporter. Because as DNA is translocated across the inner membrane
116 there should no longer be a DNA substrate for ComEA-mCherry to bind to in the periplasm,
117 thus, resulting in the resolution of ComEA-mCherry foci (**Fig. 2A**). For this assay, it was critical
118 to prevent cells from taking up any new tDNA, which would confound the ability to look at the
119 resolution of ComEA-mCherry foci due to DNA translocation across the inner membrane. So
120 after incubating cells with tDNA for 30 mins to allow for tDNA uptake into the periplasm, cells
121 were treated with DNAse to prevent any additional tDNA uptake. Then, cells were incubated for
122 2 additional hours to allow for DNA translocation across the inner membrane. When we
123 performed this experiment, we saw that the number of cells with ≥2 ComEA-mCherry foci was
124 significantly reduced in the parent but not in the Δ*comEC* mutant. This is consistent with tDNA
125 translocating across the inner membrane in the parent but not in the Δ*comEC* mutant, as
126 expected. In this assay, the Δ*sbcB* mutant was indistinguishable from the parent, suggesting
127 that SbcB does not facilitate the translocation of tDNA across the inner membrane.
128
129 *SbcB does not facilitate branch migration during NT*
130 Because SbcB was not required for the translocation of tDNA into the cytoplasm, we
131 hypothesized that it was playing a role in the downstream process of tDNA integration. Our prior
132 work demonstrates that following RecA-dependent strand invasion, the NT-specific helicase
133 ComM facilitates branch migration of tDNA into the genome (19). An unusual property of ComM
134 is that it exhibits bidirectional helicase activity and can translocate either 5'→3' or 3'→5' on DNA
135 substrates *in vitro* (19). This bidirectional helicase activity, if stochastic, would be equally likely
136 to promote or inhibit tDNA integration during NT. From experiments tracking the spatiotemporal
137 dynamics of tDNA integration in single cells, however, it is clear that ComM promotes highly
138 efficient homologous recombination during NT (17). This suggests that there may be additional
139 factors *in vivo* that promote ComM directionality. Thus, we hypothesized that the exonuclease
140 activity of SbcB may facilitate NT by regulating the directionality of ComM-dependent branch
141 migration. Specifically, that SbcB degrades the genomic strand displaced by the integrating
142 tDNA so that ComM branch migration can only proceed in one direction.
143
144 To test this, we used a previously established assay to assess branch migration activity *in vivo*
145 (19). This assay detects branch migration indirectly via assessing the comigration of two linked
146 genetic markers. Specifically, between a Trimethoprim resistance marker (Tm^R) and a nonsense
147 mutation (*i.e.*, a premature stop codon) in *lacZ*, which we refer to as *lacZ** (**Fig. 3A**). We used
148 two different tDNA products: one where Tm^R and *lacZ** are separated by 243 bp, and another
149 where they are separated by 820 bp.
150
151 Cells are transformed with this linear tDNA and if branch migration is efficient, both markers are
152 integrated into the genome. But if branch migration is inefficient, then cells may integrate the

153 Tm^R marker (which is selected for in the experiment), but not the genetically linked *lacZ**
154 mutation. When we assess the transformation frequency of the Tm^R marker in these
155 experiments, we find that Δ*sbcB* and Δ*comM* are significantly attenuated compared to the
156 parent, which is consistent with SbcB and ComM both playing an important role during NT (**Fig.**
157 **3B**). When we assess the associated comigration (*i.e.*, the linkage with the *lacZ** mutation), we
158 find that Δ*comM* is significantly reduced compared to the parent, which is consistent with the
159 established role for ComM in branch migration during NT (**Fig. 3C**). However, the comigration of
160 Δ*sbcB* is indistinguishable from the parent, despite the reduced transformation frequency in this
161 background (**Fig. 3B-C**). This suggests that SbcB may not facilitate branch migration as
162 hypothesized.
163
164 To further test this, we assessed the transformation frequency of a Δ*sbcB* Δ*comM* double
165 mutant. If these proteins work together to promote branch migration, we would expect the
166 transformation frequency of this double mutant to be similar to the single Δ*comM* or Δ*sbcB*
167 mutant (*i.e.*, an epistasic interaction). But if these genes do not act together, then we would
168 expect the transformation phenotype of Δ*sbcB* Δ*comM* to be the sum of the transformation
169 deficits observed in each single mutant. When we performed this experiment using linear tDNA,
170 we find that the reduction in NT in Δ*comM* Δ*sbcB* double mutant is the sum of the transformation
171 defects observed in Δ*comM* and Δ*sbcB* single mutants (**Fig. 3D**). These results further suggest
172 that SbcB and ComM act at distinct steps during NT. Thus, SbcB does not facilitate branch
173 migration during NT.
174
175 *SbcB acts upstream of ComM-dependent branch migration*
176 Our data thus far show that SbcB acts downstream of DNA uptake into the cytoplasm. And that
177 SbcB does not work with ComM to facilitate branch migration. To continue to narrow down
178 where SbcB acts during NT, we next sought to determine whether SbcB acts upstream or
179 downstream of ComM-dependent branch migration. We have previously demonstrated that a
180 fluorescent translational fusion of ComM (GFP-ComM) dynamically forms foci in a manner that
181 is dependent on RecA-mediated strand invasion (17). Thus, tracking the formation of GFP-
182 ComM foci demarcates cells that are actively undergoing branch migration during NT (**Fig. 4A**).
183 To test whether SbcB acted upstream of ComM-dependent branch migration, we assessed
184 GFP-ComM focus formation in the parent and Δ*sbcB* by epifluorescence timelapse microscopy.
185 We found that the percentage of cells that exhibited a GFP-ComM focus, and the number of
186 GFP-ComM foci generated in those cells was significantly lower in the Δ*sbcB* mutant compared
187 to the parent (**Fig. 4B-C**). These results suggest that SbcB is acting upstream of ComM-
188 dependent branch migration.
189
190 *SbcB is epistatic with RecA*
191 Our data suggest that SbcB is acting downstream of DNA uptake into the cytoplasm and
192 upstream of ComM-dependent branch migration. A prerequisite for ComM-dependent branch
193 migration is RecA-mediated strand invasion (17). So next, we sought to determine whether
194 SbcB facilitates RecA-mediated strand invasion. RecA is indispensable for homologous
195 recombination. Thus, Δ*recA* is incapable of NT with linear tDNA that must integrate into the
196 genome (13, 17).
197
198 Cells can also take up replicating plasmids by NT, and these products do not require
199 homologous recombination into the host genome (19). As a result, recombination is dispensable
200 when a replicating plasmid is used as tDNA. Consistent with this, Δ*comM* exhibits no reduction
201 in NT with a replicating plasmid as tDNA compared to the parent (**Fig. 5**), which is in stark
202 contrast to when linear tDNA that must recombine into the genome is used (**Fig. 3D**). Also,
203 Δ*recA* is capable of NT with a replicating plasmid as tDNA, although this mutant does exhibit an

204 ~10-fold reduction in NT (**Fig. 5**). DprA is an essential NT protein that protects ssDNA following
205 translocation into the cytoplasm. Because DprA is critical for NT when a replicating plasmid is
206 used as tDNA, this suggests that cells are still taking up DNA via the same NT pathway in these
207 experiments (**Fig. 5**).
208
209 Similar to Δ*recA*, we observed an ~10-fold reduction in NT in the Δ*sbcB* mutant. Importantly, the
210 phenotypes of Δ*sbcB* and Δ*recA* could be complemented in these assays (**Fig. 5**). To determine
211 if SbcB and RecA work together to promote NT, we assessed the phenotype of the Δ*sbcB*
212 Δ*recA* double mutant. If these proteins do not work together to facilitate NT, we would expect
213 that these mutations are non-epistatic, which would be observed as an NT defect in the double
214 mutant that matches the product of the defects observed in each single mutant. In this case,
215 each mutant exhibits an ~1-log defect in NT, thus, for a non-epistatic interaction, the double
216 mutant should exhibit an ~2-log reduction in NT compared to the parent (**Fig. 5**, dotted line). If
217 these proteins do work together, we would expect antagonistic epistasis, which would be
218 observed as an NT defect of <2-log in the double mutant. If these proteins perform the same
219 function (*i.e.*, act redundantly), we would expect synergistic epistasis, which would be observed
220 as an NT defect of >2-log in the double mutant. When we performed this experiment, we found
221 that the double mutant exhibited an ~2-log defect in NT, which is consistent with these
222 mutations being non-epistatic (**Fig. 5**). And ectopic complementation of Δ*sbcB* Δ*recA* with either
223 *sbcB* or *recA* restored NT to the level of the corresponding single mutant (**Fig. 5**). Thus, these
224 proteins likely facilitate recombination during NT in distinct ways. While it is not clear why RecA
225 and SbcB are required for NT with a replicating plasmid tDNA (see **Discussion**), the observed
226 reduction in NT in Δ*sbcB* further suggests that SbcB is acting upstream of branch migration to
227 play a presynaptic role during this process.
228
229 *SbcB does not require its exonuclease activity to promote NT*
230 SbcB is a DnaQ family exonuclease that has a highly conserved catalytic domain (20). To test
231 whether the exonuclease activity of SbcB was required for its stimulatory effect on NT, we
232 complemented Δ*sbcB* with an ectopic copy of *sbcB* containing mutations to two invariantly
233 conserved residues within the catalytic site (*sbcB** = $sbcB^{D13AE15A}$). When we assessed NT, we
234 were very surprised to find that *sbcB** did not phenocopy Δ*sbcB* (**Fig. 6A**). In fact, the NT
235 frequency for Δ*sbcB lacZ*::*sbcB** was indistinguishable from the parent (**Fig. 6A**).
236
237 The catalytic residues of SbcB mutated to generate SbcB* are invariantly conserved among
238 DnaQ family exonucleases (20), however, we sought to more rigorously test whether these
239 mutations eliminate exonuclease activity. In *E. coli*, SbcB facilitates mismatch repair by
240 participating in the excision reaction via its exonuclease activity. This is supported by the
241 observation that 4 exonucleases, RecJ, ExoVII, ExoX, and SbcB, are redundant for mismatch
242 repair in *E. coli* where the *recJ exoVII exoX sbcB* quadruple mutant has an ~6-fold elevated rate
243 of acquiring spontaneous Rif^R mutations compared to the *recJ exoVII exoX* triple mutant (21). *V.*
244 *cholerae* does not have a homolog of ExoX, but it does encode homologs to the ssDNA
245 exonucleases RecJ, ExoVII and ExoIX. So first, we assessed whether SbcB facilitates
246 mismatch repair in *V. cholerae*. To do this, we determined the spontaneous Rif^R mutation rate in
247 a Δ*recJ* Δ*exoVII* Δ*exoIX* triple mutant vs a Δ*recJ* Δ*exoVII* Δ*exoIX* Δ*sbcB* quadruple mutant. We
248 found that the latter strain exhibited a spontaneous Rif^R rate that was ~50-fold higher (**Fig. 6B**).
249 However, the spontaneous Rif^R rate for the Δ*sbcB* single mutant was indistinguishable from the
250 parent (**Fig. 6B**). This suggests that SbcB is redundant with other exonucleases for mismatch
251 repair in *V. cholerae*, as previously observed in *E. coli* (21). This redundancy with other
252 exonucleases also suggests that it is likely the exonuclease activity of SbcB that is required for
253 mismatch repair. When we ectopically expressed *sbcB* vs *sbcB** in the Δ*recJ* Δ*exoVII* Δ*exoIX*
254 Δ*sbcB* mutant, we found that the strain complemented with wildtype *sbcB* reduced the mutation

255 rate to the level of *recJ exoVII exoX*, while the strain with *sbcB** was indistinguishable from the
256 Δ*recJ* Δ*exoVII* Δ*exoIX* Δ*sbcB* parent (**Fig. 6B**). This strongly suggests that the mutations in
257 SbcB* eliminate its exonuclease activity as hypothesized.
258
259 We also assessed ssDNA exonuclease activity more directly to further test whether the
260 mutations in SbcB* eliminate its exonuclease activity. For these assays, we generated P_{tac}-
261 overexpression constructs for SbcB and SbcB*. Then, we incubated cell lysates from these
262 strains with a 5'-end labeled ssDNA oligonucleotide. In the presence of P_{tac}-*sbcB* lysate, the
263 ssDNA probe is rapidly degraded when compared to lysate from a parent strain lacking an SbcB
264 overexpression construct (**Fig. 6C**). And the degradation products formed by the P_{tac}-*sbcB*
265 lysate resemble the degradation products formed by commercially available purified *E. coli*
266 SbcB (**Fig. 6C**). Degradation of ssDNA by P_{tac}-*sbcB** lysates, however, are indistinguishable
267 from the parent lysate. All together, these data demonstrate that the mutations used to generate
268 SbcB* eliminate its exonuclease activity.
269
270 SbcB is narrowly conserved among gammaproteobacteria (22), and it has predominantly been
271 studied and characterized in the model organism *E. coli*. SbcB from *V. cholerae* is well-
272 conserved to its *E. coli* homolog (59% identity, 74% similarity). To test whether *V. cholerae*
273 SbcB has unique properties that allow it to facilitate NT, we complemented the Δ*sbcB* mutant by
274 ectopically expressing *E. coli sbcB* ($sbcB_{Ec}$). We found that $SbcB_{Ec}$ could fully complement the
275 Δ*sbcB* mutant as it restored NT back to parent levels (**Fig. 6A**). Furthermore, a catalytic mutant
276 of $SbcB_{Ec}$ ($sbcB_{Ec}$* = $sbcB_{Ec}^{D15AE17A}$) also fully restored the NT of Δ*sbcB* back to parent levels
277 (**Fig. 6A**). All together, these results indicate that the exonuclease activity of SbcB is not
278 required to facilitate NT, and that this is activity is not a unique property of *V. cholerae* SbcB.
279
280 *SbcB interacts with RecA*
281 Our data suggest that SbcB is likely facilitating RecA-dependent strand invasion in a manner
282 that does not rely on its exonuclease activity. One possibility is that SbcB directly interacts with
283 RecA to help coordinate its activity and promote recombination. To test this, we performed
284 Bacterial Adenylate Cyclase Two Hybrid (BACTH) assays (23) to assess the interaction
285 between SbcB* and RecA. When we performed these assays, we found that SbcB* exhibited
286 interactions with itself and RecA (**Fig. 7**). Because SbcB and RecA can both bind to ssDNA, this
287 interaction may not reflect a direct interaction between these proteins, but could instead
288 represent an interaction that is bridged by a ssDNA substrate in the cell. To test this, we also
289 performed BACTH analysis with DprA, which is also a ssDNA-binding protein (5). If ssDNA was
290 helping to bridge interactions in our BACTH assays, we hypothesized that we should also
291 observe interactions between SbcB* and DprA. However, when we tested this, no interactions
292 were observed between SbcB* and DprA (**Fig. 7**). This suggests that the interactions observed
293 between SbcB* and RecA are specific.
294
295
296 **DISCUSSION**
297 Our results demonstrate that SbcB acts downstream of tDNA uptake and upstream of ComM-
298 dependent branch migration. Also, they show that the exonuclease activity of SbcB is
299 dispensable for its role in promoting NT. These results help to narrow down the potential role
300 that SbcB plays during NT.
301
302 Prior work demonstrates that mutant alleles of SbcB with diminished exonuclease activity can
303 protect 3' ends (24, 25). Also, single-stranded binding protein (SSB) directly interacts with SbcB
304 to promote its exonuclease activity (26). During NT, tDNA is coated with DprA, which can evict
305 SSB and promote the loading of RecA (5). So, SSB may be excluded from interacting with SbcB

306 at the 3' end of the tDNA, which may hamper SbcB exonuclease activity during NT *in vivo*.
307 Thus, SbcB may help protect the 3' end of tDNA to facilitate recombination during NT. Our
308 observation that an exonuclease defective allele of SbcB is equally capable of promoting NT is
309 consistent with this hypothesis.
310
311 Our data demonstrate that SbcB and RecA both contribute to NT when a replicating plasmid is
312 used as the tDNA. Because ssDNA is translocated into the cytoplasm during NT, cells must
313 take up multiple independent complementary tDNA molecules to reassemble the plasmid into a
314 replicative form. In the simplest case, cells would require the uptake of 2 tDNA molecules: one
315 molecule that represents the entire ssDNA sequence of the plasmid, and a second partially
316 complementary molecule that can prime synthesis of the other strand. While RecA-dependent
317 strand invasion would not be necessary for this assembly, it is possible that RecA promotes
318 annealing of complementary sequences, resulting in the observed ~10-fold deficit for Δ*recA*
319 when a replicating plasmid is used as tDNA. Our data also showed an ~10-fold deficit for Δ*sbcB*
320 in these assays. However epistasis analysis indicated that these mutations were non-epistatic.
321 Thus, RecA and SbcB likely facilitate NT with a replicating plasmid in distinct ways. RecA may
322 facilitate annealing, while SbcB helps protect the 3' end of the tDNA.
323
324 RecA assembly on ssDNA occurs unidirectionally from 5' → 3' (27). Thus, for RecA to bind to
325 the 3' end of a long tDNA molecule, it must be processively assembled from an upstream 5' site.
326 As a 3' → 5' exonuclease, SbcB binds to the 3' ends of ssDNA molecules. Our results provide
327 preliminary genetic evidence that SbcB directly interacts with RecA, which may help recruit
328 RecA to the 3' end of single-stranded tDNA. When a linear tDNA homologous to the host
329 chromosome is used, RecA loading on the 3' end could also facilitate homologous
330 recombination by promoting strand invasion of the 3' end into the genome. This could allow the
331 integrated 3' end to initiate DNA replication, which would stabilize the recombination
332 intermediate (28). Interestingly, prior data suggest that SbcB facilitates RecA-dependent
333 recombination *in vitro* (29). In these studies, however, it was presumed that this stimulatory
334 effect of SbcB was due to its exonuclease activity.
335
336 SbcB has primarily been characterized in *E. coli*, and a number of studies have noted distinct
337 recombination phenotypes in exonuclease defective alleles of *sbcB* (*i.e.*, *sbcB15*) vs *sbcB* null
338 mutants (*i.e.*, Δ*sbcB* and *xonA2*) (24, 30, 31). These studies suggest that SbcB has an activity
339 that facilitates recombination beyond its exonuclease activity. Consistent with what is observed
340 in *E. coli*, we uncover a phenotype for SbcB in *V. cholerae* that is distinct from its exonuclease
341 activity. Interestingly, revealing these phenotypes for SbcB in *E. coli* relied on genetic
342 backgrounds that lack other recombination proteins like RecBCD and SbcCD (24, 30, 31), while
343 in *V. cholerae* we observe this phenotype even when these recombination factors are intact.
344 Regardless, these results suggest that an exonuclease independent activity of SbcB may be
345 conserved. Indeed, this is supported by our observation that *E. coli* SbcB can complement the
346 NT defect of a *V. cholerae* Δ*sbcB* mutant. It is tempting to speculate that this exonuclease-
347 independent activity is due to SbcB-RecA interactions, which we provide preliminary genetic
348 evidence for here.
349
350 All together, these results elucidate a new role for the canonical exonuclease SbcB in facilitating
351 the integration of tDNA during horizontal gene transfer by NT in *V. cholerae*. Future work will
352 focus on testing on testing SbcB-RecA interactions biochemically and the impact of these
353 interactions on recombination both *in vitro* and *in vivo*. While NT is broadly conserved in diverse
354 microbial species (32), SbcB is narrowly conserved among gammaproteobacteria (22). So it is
355 tempting to speculate that the role that SbcB plays during NT in *V. cholerae*, is facilitated by
356 other recombination proteins in more distantly related naturally transformable species.

357
358
359 **METHODS**
360 *Bacterial Strains and Culture Conditions*
361 All strains were derived from *V. cholerae* E7946 (33). Cells were routinely grown in LB Miller
362 broth and agar supplemented with spectinomycin (200 µg/mL), kanamycin (50 µg/mL),
363 trimethoprim (10 µg/mL), tetracycline (0.5 µg/mL), sulfamethoxazole (100 µg/mL),
364 chloramphenicol (1 µg/mL), erythromycin (10 µg/mL), carbenicillin (20 µg/mL), or zeocin (100
365 µg/mL) as appropriate.
366
367 *Construction of mutant strains*
368 All strains were generated by natural transformation / MuGENT using splicing-by-overlap-
369 extension (SOE) PCR mutant constructs exactly as previously described (34, 35). Ectopic
370 expression constructs were generated by SOE PCR and integrated onto the *V. cholerae*
371 genome exactly as previously described (36). All strains were confirmed by PCR and/or
372 sequencing. For a detailed list of all mutants used in this study, see **Table S1.** For a complete
373 list of primers used to generate mutant constructs, see **Table S2**.
374
375 *Natural transformation assays*
376 As discussed in the text, cells were engineered to bypass the native signals required for NT in
377 *V. cholerae*. Specifically, the master competence regulator TfoX was overexpressed via an
378 isopropyl β-d-1-thiogalactopyranoside (IPTG)-inducible P_{tac} promoter, and the cells are
379 genetically locked in a high cell density state via deletion of *luxO*, as previously described .
380 Chitin-independent transformation assays to determine NT frequency were performed exactly
381 as previously described (1). Briefly, cells were grow at 30ºC rolling in LB supplemented with 100
382 µM IPTG, 20 mM $MgCl_2$, 10 mM $CaCl_2$ to late-log. Then, ~10^8 CFUs were diluted into instant
383 ocean medium (7g/L; Aquarium Systems). Next, transforming DNA (tDNA) was added into each
384 reaction as appropriate. For linear tDNA that must integrate into the genome, 100 ng of a
385 ΔVC1807::Erm^R product was used. VC1807 is a frame-shifted transposase gene. For replicating
386 plasmid as tDNA, pBAD18-Kan (37) was miniprepped from *E. coli* TG1. Control reactions were
387 performed for each strain where no tDNA was added. Cells were incubated with tDNA
388 overnight. Then, reactions were outgrown by adding 1mL of LB and shaking at 37ºC for 3 hours.
389 Reactions were then plated for quantitative culture by dribble plating on LB agar supplemented
390 with the appropriate antibiotic to quantify transformants, and plain LB to quantify total viable
391 counts. Transformation frequency is defined as the CFU/mL of transformants divided by the
392 CFU/mL of total viable counts.
393
394 For assays where branch migration was indirectly assessed via linkage analysis, transformation
395 reactions were performed exactly as described above except that they were plated onto LB agar
396 supplemented with trimethoprim and X-gal (40 µg/mL). On these plates, all cells integrated the
397 Tm^R marker, and if cells integrated the genetically linked *lacZ* nonsense mutation they would
398 make white colonies. If they did not integrate the linked lacZ nonsense mutation, they would
399 make blue colonies on these plates. Thus, the comigration frequency is defined as the percent
400 of Tm^R colonies that were white on these plates.
401
402 *Spontaneous Rif^R mutant frequency assays*
403 All strains were isolation streak plated onto plain LB agar. Then, single colonies were picked
404 and grown overnight in plain LB. These cultures were then concentrated and ~10^{10} CFUs were
405 spread onto LB agar plates supplemented with Rifampicin 100 µg/mL to quantify Rif^R mutants.
406 Concentrated cultures were also dilution dribble plated onto plain LB agar plates to quantify total
407 CFU. The Rif^R mutant frequency is defined as Rif^R CFU / total CFU.

408
409 *Microscopy*
410 Phase contrast and fluorescence images were collected on a Nikon Ti-2 microscope using a
411 Plan Apo × 60 objective, a YFP and/or mCherry filter cube, a Hamamatsu ORCA Flash 4.0
412 camera and Nikon NIS Elements imaging software.
413
414 To assess ComEA-mCherry localization upon DNA uptake, cells were grown to induce
415 competence as described above for natural transformation assays. Then, ~10^7 cells were mixed
416 with ~750 ng of a 6kb PCR product as tDNA. Reactions were incubated at 30ºC static for 30
417 mins to allow for tDNA uptake into the periplasm. Half the reaction was then placed on ice for
418 imaging at this time point. DNAse was added to the other half of the reaction, which was then
419 incubated at 37ºC for 120 mins. Then, both samples (30 min and 150 min) were placed under
420 0.2% gelzan pads and imaged. The number of ComEA-mCherry foci was determined by
421 analyzing 60 cells per replicate.
422
423 To assess GFP-ComM focus formation, cells were grown to induce competence as described
424 above for natural transformation assays. Then, ~10^7 cells were mixed with ~650 ng of a 6kb
425 tDNA product that will integrate into the genome, and placed under an 0.2% gelzan pad.
426 Samples were then subjected to timelapse imaging where images were taken every 2 min for 3
427 hours. The number of GFP-ComM foci was determined by analyzing 60 cells per replicate.
428
429 *ssDNA exonuclease activity assays*
430 Strains were grown overnight in LB supplemented with 1 mM IPTG. Then, cells were washed
431 and concentrated to an OD_{600} = 25.0 in Buffer A: 10mM Tris pH 7.5, 100 mM NaCl. Then, the
432 following reagents were added to the indicated final concentrations to lyse cells: 1x FastBreak
433 cell lysis reagent (Promega), 100 µg/mL lysozyme, 1 mM PMSF, 1x protease inhibitor cocktail,
434 and 10 mM beta-mercaptoethanol. The 100x inhibitor cocktail contained the following: 0.07
435 mg/mL phosphoramidon (Santa Cruz), 0.006 mg/mL bestatin (MPbiomedicals/Fisher Scientific),
436 1.67 mg/mL AEBSF (Gold Bio), 0.07 mg/mL pepstatin A (DOT Scientific), 0.07 mg/mL E64
437 (Gold Bio) suspended in DMSO). Next, samples were subjected to bead beating with lysing
438 matrix B on a FastPrep-24 instrument (MP Bio) with 3 x 40 s pulses at 6.0 m/s. Lysates were
439 centrifuged at 18,000 x g for 2 mins and the supernatant was transferred to a fresh eppi. The
440 ssDNA probe used was PP327 (kindly provided by Payel Paul and Julia van Kessel), a 5'
441 IR800CW end-labeled oligonucleotide (see **Table S2**). Next, 20 µL ssDNA exonuclease
442 reactions were setup as follows: 3 µL PP327 (2 µM), 2 µL 10X Exonuclease I reaction buffer
443 (NEB), 13 µL water, and 2 µL of cell lysate. Negative control reactions were performed where
444 lysate was substituted with 2 µL of Buffer A. And a positive control reaction was performed
445 where lysate was substituted with 2 µL (20 U) of purified Exonuclease I (NEB). Reactions were
446 allowed to incubate for 1 min at room temperature. Then, 2 µL of each sample was mixed with 8
447 µL of 1.25X formamide loading buffer (90% formamide, 37.5 mM EDTA pH 8.0, 2 mg/mL orange
448 G) to stop reactions. Next, samples were electrophoretically separated on a prerun Tris Borate
449 EDTA (TBE)-Urea gel (15% 29:1 acrylamide/bis-acrylamide; 8M Urea) in 1X TBE at 200 V. Gels
450 were then imaged on a Protein Simple FluorChem R instrument on the infrared setting to
451 visualize the IR800 labeled probe.
452
453 *Bacterial Adenylate Cyclase Two-Hybrid (BACTH) Assays*
454 Gene inserts were amplified by PCR and cloned into the pUT18C, pUT18, pKT25, or pKNT25
455 vectors to generate N- and C- terminal fusions to the T18 and T25 fragments of adenylate
456 cyclase. Miniprepped vectors were then cotransformed into *E. coli* BTH101 and outgrown with
457 500 µL LB for 1 hour at 37°C with shaking. Reactions were plated on LB agar plates
458 supplemented with kanamycin 50 µg/mL and carbenicillin 100 µg/mL to select for transformants

459 that received both plasmids. Single colonies were then picked and grown statically at 30°C in LB
460 supplemented with kanamycin 50 µg/mL and carbenicillin 100 µg/mL. Then, 3 µL of each strain
461 was spotted onto LB agar plates supplemented with kanamycin 50 µg/mL, carbenicillin
462 100µg/mL, 0.5 mM IPTG and 40 µg/mL X-gal. Plates were incubated at 30°C for 24 hours prior
463 to imaging on an Epson Perfection V600 scanner.
464
465 *Statistics*
466 Statistical differences were assessed using GraphPad Prism software. The statical tests
467 employed are indicated in figure legends. Descriptive statistics for all samples, and a
468 comprehensive list of statistical comparisons can be found in **Dataset S1**.
469
470
471 **ACKNOWLEDGEMENTS**
472 This work was supported by grant R35GM128674 from the National Institutes of Health to ABD.
473
474
475 **REFERENCES**
476
477 1. Ellison CK, Dalia TN, Vidal Ceballos A, Wang JC, Biais N, Brun YV, Dalia AB. 2018.
478 Retraction of DNA-bound type IV competence pili initiates DNA uptake during natural
479 transformation in Vibrio cholerae. Nat Microbiol 3:773-780.
480 2. Dubnau D, Blokesch M. 2019. Mechanisms of DNA Uptake by Naturally Competent
481 Bacteria. Annu Rev Genet 53:217-237.
482 3. Gangel H, Hepp C, Muller S, Oldewurtel ER, Aas FE, Koomey M, Maier B. 2014.
483 Concerted spatio-temporal dynamics of imported DNA and ComE DNA uptake protein
484 during gonococcal transformation. PLoS Pathog 10:e1004043.
485 4. Seitz P, Pezeshgi Modarres H, Borgeaud S, Bulushev RD, Steinbock LJ, Radenovic A,
486 Dal Peraro M, Blokesch M. 2014. ComEA is essential for the transfer of external DNA
487 into the periplasm in naturally transformable Vibrio cholerae cells. PLoS Genet
488 10:e1004066.
489 5. Mortier-Barriere I, Velten M, Dupaigne P, Mirouze N, Pietrement O, McGovern S,
490 Fichant G, Martin B, Noirot P, Le Cam E, Polard P, Claverys JP. 2007. A key
491 presynaptic role in transformation for a widespread bacterial protein: DprA conveys
492 incoming ssDNA to RecA. Cell 130:824-36.
493 6. Dalia TN, Yoon SH, Galli E, Barre FX, Waters CM, Dalia AB. 2017. Enhancing multiplex
494 genome editing by natural transformation (MuGENT) via inactivation of ssDNA
495 exonucleases. Nucleic Acids Res 45:7527-7537.
496 7. Lehman IR. 1960. The deoxyribonucleases of Escherichia coli. I. Purification and
497 properties of a phosphodiesterase. J Biol Chem 235:1479-87.
498 8. Kushner SR, Nagaishi H, Templin A, Clark AJ. 1971. Genetic recombination in
499 Escherichia coli: the role of exonuclease I. Proc Natl Acad Sci U S A 68:824-7.
500 9. Kushner SR, Nagaishi H, Clark AJ. 1972. Indirect suppression of recB and recC
501 mutations by exonuclease I deficiency. Proc Natl Acad Sci U S A 69:1366-70.
502 10. Meibom KL, Blokesch M, Dolganov NA, Wu CY, Schoolnik GK. 2005. Chitin induces
503 natural competence in Vibrio cholerae. Science 310:1824-7.
504 11. Lo Scrudato M, Blokesch M. 2012. The regulatory network of natural competence and
505 transformation of Vibrio cholerae. PLoS Genet 8:e1002778.
506 12. Bassler BL, Wright M, Silverman MR. 1994. Sequence and function of LuxO, a negative
507 regulator of luminescence in Vibrio harveyi. Mol Microbiol 12:403-12.
508 13. Seitz P, Blokesch M. 2013. DNA-uptake machinery of naturally competent Vibrio
509 cholerae. Proc Natl Acad Sci U S A 110:17987-92.

14. Weaver SJ, Ortega DR, Sazinsky MH, Dalia TN, Dalia AB, Jensen GJ. 2020. CryoEM structure of the type IVa pilus secretin required for natural competence in Vibrio cholerae. Nat Commun 11:5080.
15. Lacks S. 1962. Molecular fate of DNA in genetic transformation of Pneumococcus. J Mol Biol 5:119-31.
16. Inamine GS, Dubnau D. 1995. ComEA, a Bacillus subtilis integral membrane protein required for genetic transformation, is needed for both DNA binding and transport. J Bacteriol 177:3045-51.
17. Dalia AB, Dalia TN. 2019. Spatiotemporal Analysis of DNA Integration during Natural Transformation Reveals a Mode of Nongenetic Inheritance in Bacteria. Cell 179:1499-1511 e10.
18. Seitz P, Blokesch M. 2014. DNA transport across the outer and inner membranes of naturally transformable Vibrio cholerae is spatially but not temporally coupled. MBio 5:e01409-14.
19. Nero TM, Dalia TN, Wang JC, Kysela DT, Bochman ML, Dalia AB. 2018. ComM is a hexameric helicase that promotes branch migration during natural transformation in diverse Gram-negative species. Nucleic Acids Res 46:6099-6111.
20. Fijalkowska IJ, Schaaper RM. 1996. Mutants in the Exo I motif of Escherichia coli dnaQ: defective proofreading and inviability due to error catastrophe. Proc Natl Acad Sci U S A 93:2856-61.
21. Viswanathan M, Burdett V, Baitinger C, Modrich P, Lovett ST. 2001. Redundant exonuclease involvement in Escherichia coli methyl-directed mismatch repair. J Biol Chem 276:31053-8.
22. Lovett ST. 2011. The DNA Exonucleases of Escherichia coli. EcoSal Plus 4.
23. Karimova G, Pidoux J, Ullmann A, Ladant D. 1998. A bacterial two-hybrid system based on a reconstituted signal transduction pathway. Proc Natl Acad Sci U S A 95:5752-6.
24. Thoms B, Borchers I, Wackernagel W. 2008. Effects of single-strand DNases ExoI, RecJ, ExoVII, and SbcCD on homologous recombination of recBCD+ strains of Escherichia coli and roles of SbcB15 and XonA2 ExoI mutant enzymes. J Bacteriol 190:179-92.
25. Razavy H, Szigety SK, Rosenberg SM. 1996. Evidence for both 3' and 5' single-strand DNA ends in intermediates in chi-stimulated recombination in vivo. Genetics 142:333-9.
26. Lu D, Myers AR, George NP, Keck JL. 2011. Mechanism of Exonuclease I stimulation by the single-stranded DNA-binding protein. Nucleic Acids Res 39:6536-45.
27. Cox MM, Lehman IR. 1981. Directionality and polarity in recA protein-promoted branch migration. Proc Natl Acad Sci U S A 78:6018-22.
28. Gupta RC, Golub EI, Wold MS, Radding CM. 1998. Polarity of DNA strand exchange promoted by recombination proteins of the RecA family. Proc Natl Acad Sci U S A 95:9843-8.
29. Konforti BB, Davis RW. 1992. ATP hydrolysis and the displaced strand are two factors that determine the polarity of RecA-promoted DNA strand exchange. J Mol Biol 227:38-53.
30. Buljubasic M, Hlevnjak A, Repar J, Dermic D, Filic V, Weber I, Zahradka K, Zahradka D. 2019. RecBCD- RecFOR-independent pathway of homologous recombination in Escherichia coli. DNA Repair (Amst) 83:102670.
31. Zahradka K, Simic S, Buljubasic M, Petranovic M, Dermic D, Zahradka D. 2006. sbcB15 And DeltasbcB mutations activate two types of recf recombination pathways in Escherichia coli. J Bacteriol 188:7562-71.
32. Lorenz MG, Wackernagel W. 1994. Bacterial gene transfer by natural genetic transformation in the environment. Microbiol Rev 58:563-602.

33. Miller VL, DiRita VJ, Mekalanos JJ. 1989. Identification of toxS, a regulatory gene whose product enhances toxR-mediated activation of the cholera toxin promoter. J Bacteriol 171:1288-93.
34. Dalia AB. 2018. Natural Cotransformation and Multiplex Genome Editing by Natural Transformation (MuGENT) of Vibrio cholerae. Methods Mol Biol 1839:53-64.
35. Dalia AB, McDonough E, Camilli A. 2014. Multiplex genome editing by natural transformation. Proc Natl Acad Sci U S A 111:8937-42.
36. Dalia TN, Chlebek JL, Dalia AB. 2020. A modular chromosomally integrated toolkit for ectopic gene expression in Vibrio cholerae. Sci Rep 10:15398.
37. Guzman LM, Belin D, Carson MJ, Beckwith J. 1995. Tight regulation, modulation, and high-level expression by vectors containing the arabinose PBAD promoter. J Bacteriol 177:4121-30.

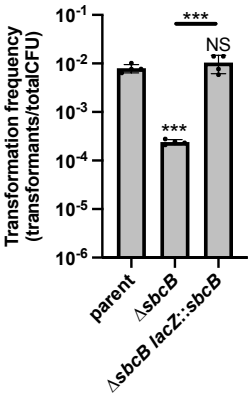

Fig. 1. **SbcB facilitates NT in *Vibrio cholerae.*** Natural transformation assays of the indicated strains. Data are from four independent biological replicates and shown as the mean ± SD. Statistical comparisons were made by one-way ANOVA with Tukey's multiple comparison test of the log-transformed data. NS, not significant. *** = $p < 0.001$

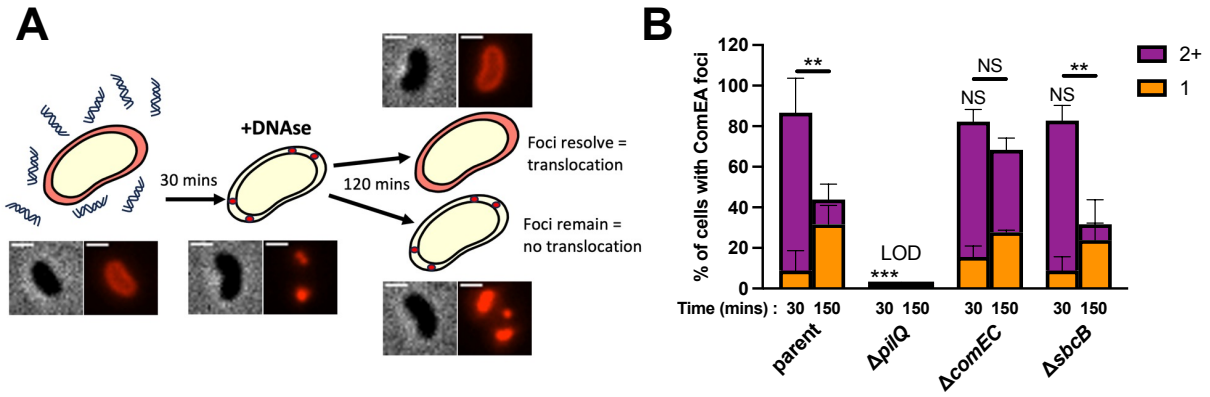

Fig. 2. **SbcB does not affect DNA uptake during NT.** (**A**) Schematic and representative images of the experimental setup used to assess DNA uptake during NT. Cells contained a ComEA-mCherry fusion and were incubated with tDNA. The presence of a ComEA-mCherry focus indicates that tDNA is taken up into the periplasm. After 30 mins, DNAse was added to remove all extracellular DNA. The subsequent tracking of ComEA-mCherry foci was used as an indirect readout to demarcate the translocation of periplasmic tDNA into the cytoplasm. Scale bar, 1 µm. (**B**) The assay described in **A** was performed in the indicated strain backgrounds and the frequency of cells with 1 or more than 1 (2+) ComEA-mCherry foci is reported at the indicated time points. Data are from 3 independent biological replicates and shown as the mean ± SD; n = 180 cells analyzed in each strain background. Statistical comparisons for the frequencies of cells with 2+ ComEA-mCherry foci were made by one-way ANOVA with Tukey's multiple comparison test of the log-transformed data. LOD, limit of detection. NS, not significant. ** = $p < 0.01$

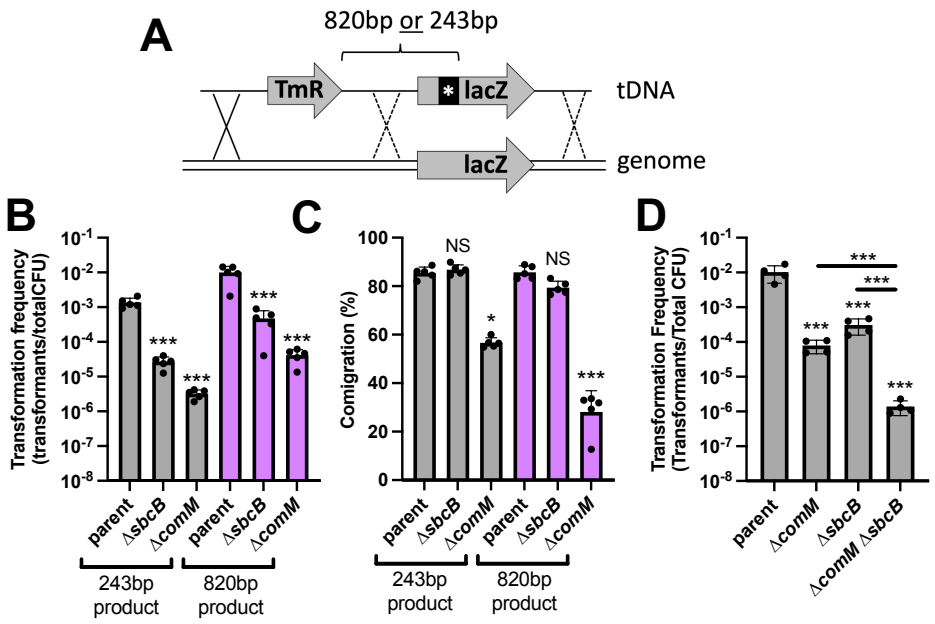

Fig. 3. **SbcB does not promote ComM-dependent branch migration.** (**A**) Schematic of the experimental setup to assess branch migration via linkage analysis between a trimethoprim resistance marker (Tm^R) and a nonsense mutation in *lacZ*. Two different tDNAs were used: one where the *lacZ* nonsense mutation was 243 bp away from the Tm^R cassette, and another where the spacing was 820 bp. The two tDNA products described in **A** were naturally transformed into the indicated strains and the (**B**) transformation frequency and (**C**) comigration frequency (i.e., the frequency of linkage between the Tm^R and *lacZ* nonsense mutation) are reported. All strains in these assays contained a Δ*mutS* mutation to prevent mismatch repair from confounding the results. (**D**) Natural transformation assays of the indicated strains. All data are from at least 4 independent biological replicates and shown as the mean ± SD. Statistical comparisons were made by one-way ANOVA with Tukey's multiple comparison test of the log-transformed data. NS, not significant. *** = $p < 0.001$, ** = $p < 0.01$, * = $p < 0.05$. Statistical identifiers directly above bars represent comparisons to the parent.

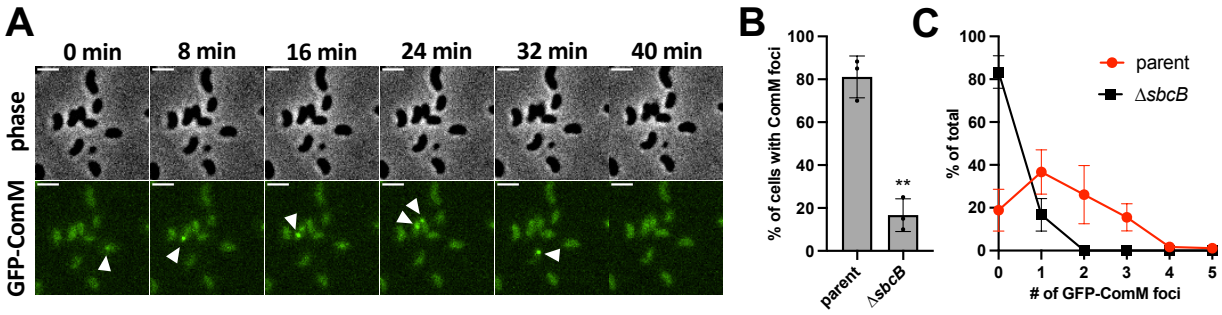

Fig. 4. **SbcB acts upstream of ComM-dependent branch migration.** (**A**) Montage of timelapse imaging of cells expressing a GFP-ComM fluorescent fusion incubated with tDNA. White arrows indicate the appearance of transient GFP-ComM foci. Scale bar, 2 µm. Experiments were performed as in **A** in the parent and Δ*sbcB* background to quantify the (**B**) proportion of cells that exhibited any GFP-ComM foci and the (**C**) distribution of the GFP-ComM foci observed. Data are from 3 independent biological replicates and shown as the mean ± SD; n = 180 cells analyzed in each strain background. Statistical comparison in **B** was made by unpaired Student's t-test of the log-transformed data. ** = $p < 0.01$. Statistical identifier directly above bar represents comparisons to the parent.

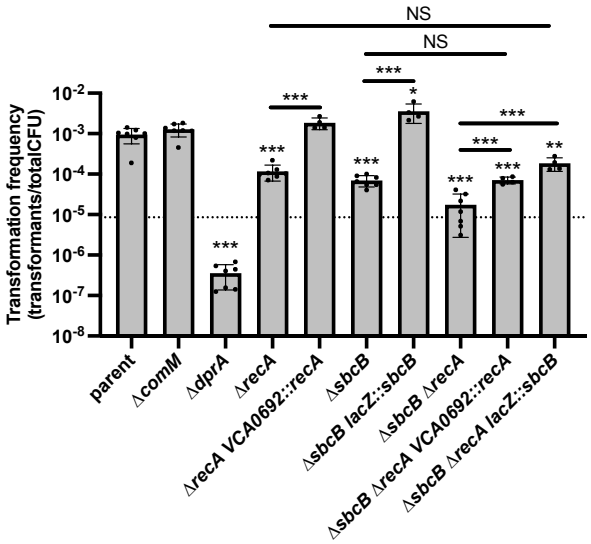

Fig. 5. **SbcB and RecA facilitate NT when a replicating plasmid is used as the tDNA but are non-epistatic.** Natural transformation assays of the indicated strains using a replicating plasmid as the tDNA. Data are from at least 4 independent biological replicate and shown as the mean ± SD. Statistical comparisons were made by one-way ANOVA with Tukey's multiple comparison test of the log-transformed data. NS, not significant. *** = $p < 0.001$, ** = $p < 0.01$, * = $p < 0.05$. The dotted line represents the expected phenotype for Δ*sbcB* Δ*recA* if these mutations are non-epistatic. Statistical identifiers directly above bars represent comparisons to the parent.

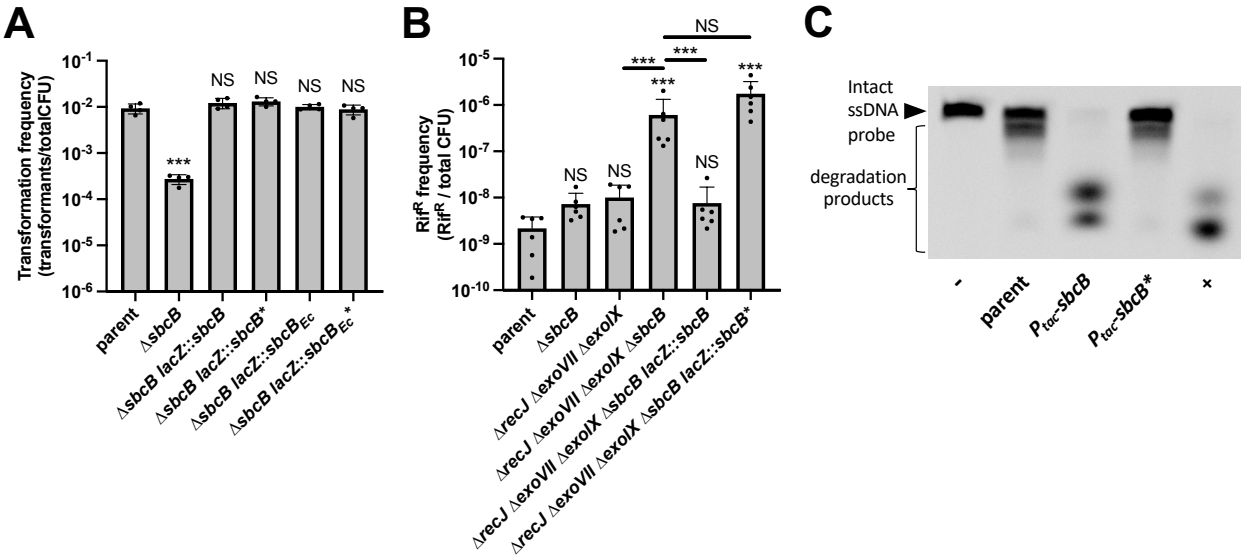

Fig. 6. **SbcB facilitates NT in *Vibrio cholerae* independent of its exonuclease activity.** (**A**) Natural transformation assays of the indicated strains using linear tDNA. (**B**) Quantifying the frequency of spontaneous Rif^R mutants in the indicated strain backgrounds. All data in **A** and **B** are from at least 4 independent biological replicates and shown as the mean ± SD. NS, not significant. *** = $p < 0.001$. Statistical identifiers directly above bars represent comparisons to the parent. (**C**) Exonuclease activity assay using cell lysates from the indicated strains. All strains were grown overnight in 1 mM IPTG for these assays. "-" denotes a reaction where no lysate was added, while "+" denotes a sample where purified SbcB (*i.e.*, NEB Exonuclease I) was added. Data are representative of two independent experiments.

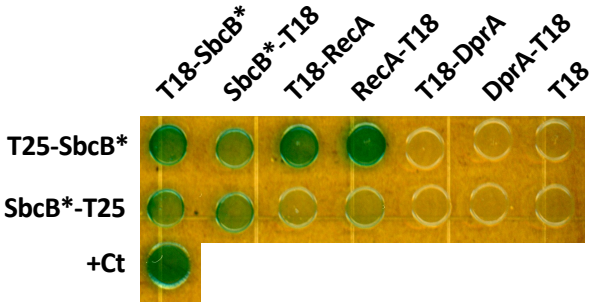

Fig. 7. **SbcB interacts with RecA.** Bacterial Adenylate Cyclase Two-Hybrid (BACTH) assays were performed to assess pairwise interactions between SbcB* (SbcB* = the $SbcB^{D13A,E15A}$ catalytic mutant) and RecA or DprA. The indicated proteins were fused to the T18 or T25 fragments of adenylate cyclase as indicated. Leucine zipper fusions to T18 and T25 served as a positive control for interacting proteins (+Ct). Data are representative of 3 independent biological replicates.

658 **Table S1** - *Strains used in this study*
659

Strain #*	Genotype	Figures	Use in manuscript
SAD030	*V. cholerae* E7946 Sm^R	Fig. 6B	parent for all strains in this study, and the parent for spontaneous Rif^R mutant frequency assays
TND0905 / SAD2468	P_{tac}-*tfoX*, Δ*luxO, lacZ*::*lacI*^{q}, *pilA*^{S67C}, Δ*VC1807*::*Zeo*^{R}	Fig. 1, 3D, 5, 6A, 6C	parent for NT frequency assays and ssDNA exonuclease activity assays
TND4174 / SAD3565	Δ*sbcB*::*Tm*^{R}, P_{tac}-*tfoX*, Δ*luxO, lacZ*::*lacI*^{q}, *pilA*^{S67C}, Δ*VC1807*::*Zeo*^{R}	Fig. 1, 3D, 5, 6A	Δ*sbcB* for NT frequency assays
TND4301 / SAD3566	Δ*lacZ*::*Spec*^{R}-P_{native}-*sbcB*, Δ*sbcB*::*Tm*^{R}, P_{tac}-*tfoX*, Δ*luxO*, *pilA*^{S67C}, Δ*VC1807*::*Zeo*^{R}	Fig. 1, 6A	Δ*sbcB lacZ*::*sbcB* for NT frequency assays
TND2245 / SAD3567	Δ*comM*::*Carb*^{R}, P_{tac}-*tfoX*, Δ*luxO, lacZ*::*lacI*^{q}, *pilA*^{S67C}, Δ*VC1807*::*Zeo*^{R}	Fig. 3D, 5	Δ*comM* for NT frequency assays
TND4175 / SAD3568	Δ*sbcB*::*Tm*^{R}, Δ*comM*::*Carb*^{R}, P_{tac}-*tfoX*, Δ*luxO, lacZ*::*lacI*^{q}, *pilA*^{S67C}, Δ*VC1807*::*Zeo*^{R}	Fig. 3D	Δ*sbcB* Δ*comM* for NT frequency assays
TND1072 / SAD3569	Δ*dprA*::*Cm*^{R}, P_{tac}-*tfoX*, Δ*luxO, lacZ*::*lacI*^{q}, *pilA*^{S67C}, Δ*VC1807*::*Zeo*^{R}	Fig. 5	Δ*dprA* for NT frequency assays
TND4543 / SAD3570	Δ*recA*::*Spec*^{R}, P_{tac}-*tfoX*, Δ*luxO, lacZ*::*lacI*^{q}, *pilA*^{S67C}, Δ*VC1807*::*Zeo*^{R}	Fig. 5	Δ*recA* for NT frequency assays
TND4542 / SAD3571	Δ*recA*::*Spec*^{R}, Δ*sbcB*::*Tm*^{R}, P_{tac}-*tfoX*, Δ*luxO, lacZ*::*lacI*^{q}, *pilA*^{S67C}, Δ*VC1807*::*Zeo*^{R}	Fig. 5	Δ*sbcB* Δ*recA* for NT frequency assays
TND4667 / SAD3622	Δ*VCA0692*::*Carb*^{R}-P_{native}-*recA*, Δ*recA*::*Spec*^{R}, P_{tac}-*tfoX*, Δ*luxO, lacZ*::*lacI*^{q}, *pilA*^{S67C}, Δ*VC1807*::*Zeo*^{R}	Fig. 5	Δ*recA VCA0692*::*recA* for NT frequency assays
TND4663 / SAD3623	Δ*lacZ*::*Cm*^{R}-P_{native}-*sbcB*, Δ*sbcB*::*Tm*^{R}, P_{tac}-*tfoX*, Δ*luxO, pilA*^{S67C}, Δ*VC1807*::*Zeo*^{R}	Fig. 5	Δ*sbcB lacZ*::*sbcB* for NT frequency assays
TND4668 / SAD3624	Δ*VCA0692*::*Carb*^{R}-P_{native}-*recA*, Δ*recA*::*Spec*^{R}, Δ*sbcB*::*Tm*^{R}, P_{tac}-*tfoX*, Δ*luxO, lacZ*::*lacI*^{q}, *pilA*^{S67C}, Δ*VC1807*::*Zeo*^{R}	Fig. 5	Δ*sbcB* Δ*recA VCA0692*::*recA* for NT frequency assays
TND4666 / SAD3625	Δ*lacZ*::*Cm*^{R}-P_{native}-*sbcB*, Δ*sbcB*::*Tm*^{R}, Δ*recA*::*Spec*^{R}, Δ*sbcB*::*Tm*^{R}, P_{tac}-*tfoX*, Δ*luxO, pilA*^{S67C}, Δ*VC1807*::*Zeo*^{R}	Fig. 5	Δ*sbcB* Δ*recA lacZ*::*sbcB* for NT frequency assays
TND4338 / SAD3572	Δ*lacZ*::*Spec*^{R}-P_{native}-*sbcB*^{D13A,E15A}, Δ*sbcB*::*Tm*^{R}, P_{tac}-*tfoX*, Δ*luxO*, *pilA*^{S67C}, Δ*VC1807*::*Zeo*^{R}	Fig. 6A	Δ*sbcB lacZ*::*sbcB** for NT frequency assays
TND4407 / SAD3573	Δ*lacZ*::*Spec*^{R}-P_{native}-*sbcB*$_{E.coli}$, Δ*sbcB*::*Tm*^{R}, P_{tac}-*tfoX*, Δ*luxO*, *pilA*^{S67C}, Δ*VC1807*::*Zeo*^{R}	Fig. 6A	Δ*sbcB lacZ*::*sbcB*$_{Ec}$ for NT frequency assays
TND4472 / SAD3574	Δ*lacZ*::*Spec*^{R}-P_{native}-*sbcB*$_{E.coli}$^{D15A,D17A}, Δ*sbcB*::*Tm*^{R}, P_{tac}-*tfoX*, Δ*luxO*, *pilA*^{S67C}, Δ*VC1807*::*Zeo*^{R}	Fig. 6A	Δ*sbcB lacZ*::*sbcB*$_{Ec}$* for NT frequency assays
TND0111 / SAD1505	Δ*sbcB*::*Kan*^{R}	Fig. 6B	Δ*sbcB* for spontaneous Rif^R mutant frequency assays
TND4599 / SAD3575	Δ*recJ*::*Zeo*^{R}, Δ*exoVII*::*Carb*^{R}, Δ*exoIX*::Kan^R	Fig. 6B	Δ*recJ* Δ*exoVII* Δ*exoIX* for spontaneous Rif^R mutant frequency assays
TND4605 / SAD3576	Δ*sbcB*::*Tm*^{R}, Δ*recJ*::*Zeo*^{R}, Δ*exoVII*::*Carb*^{R}, Δ*exoIX*::Kan^R	Fig. 6B	Δ*sbcB* Δ*recJ* Δ*exoVII* Δ*exoIX* for spontaneous Rif^R mutant frequency assays
TND4606 / SAD3577	Δ*lacZ*::*Spec*^{R}-P_{native}-*sbcB*, Δ*sbcB*::*Tm*^{R}, Δ*recJ*::*Zeo*^{R}, Δ*exoVII*::*Carb*^{R}, Δ*exoIX*::Kan^R	Fig. 6B	Δ*sbcB* Δ*recJ* Δ*exoVII* Δ*exoIX lacZ*::*sbcB* for spontaneous Rif^R mutant frequency assays

TND4607 / SAD3578	Δ*lacZ*::*Spec*^{R}-*P*$_{native}$-*sbcB*^{D13A,E15A}, Δ*sbcB*::*Tm*^{R}, Δ*recJ*::*Zeo*^{R}, Δ*exoVII*::*Carb*^{R}, Δ*exoIX*::Kan^{R}	Fig. 6B	Δ*sbcB* Δ*recJ* Δ*exoVII* Δ*exoIX* *lacZ::sbcB** for spontaneous Rif^{R} mutant frequency assays
TND4288 / SAD3626	Δ*lacZ*::*Spec*^{R}-*P*^{tac}-*sbcB*, *P*$_{tac}$-*tfoX*, Δ*luxO*, *lacZ*::*lacI*^{q}, *pilA*^{S67C}, Δ*VC1807*::*Zeo*^{R}	Fig. 6C	*P*$_{tac}$-*sbcB* for ssDNA exonuclease activity assays
TND4665 / SAD3627	Δ*lacZ*::*Spec*^{R}-*P*^{tac}-*sbcB*^{D13A,E15A}, *P*$_{tac}$-*tfoX*, Δ*luxO*, *lacZ*::*lacI*^{q}, *pilA*^{S67C}, Δ*VC1807*::*Zeo*^{R}	Fig. 6C	*P*$_{tac}$-*sbcB** for ssDNA exonuclease activity assays
TND0904 / SAD2436	*comEA-mCherry*, *P*$_{tac}$-*tfoX*, Δ*luxO*, *lacZ*::*lacI*^{q}, *pilA*^{S67C}, Δ*VC1807*::*Cm*^{R}	Fig. 2	parent for ComEA-mCherry localization assays
TND4170 / SAD3579	Δ*pilQ*::*Tet*^{R}, *comEA-mCherry*, *P*$_{tac}$-*tfoX*, Δ*luxO*, *lacZ*::*lacI*^{q}, *pilA*^{S67C}, Δ*VC1807*::*Cm*^{R}	Fig. 2	Δ*pilQ* for ComEA-mCherry localization assays
JLC645 / SAD3580	Δ*comEC*::*Kan*^{R}, *comEA-mCherry*, *P*$_{tac}$-*tfoX*, Δ*luxO*, *lacZ*::*lacI*^{q}, *pilA*^{S67C}, Δ*VC1807*::*Cm*^{R}	Fig. 2	Δ*comEC* for ComEA-mCherry localization assays
TND4173 / SAD3581	Δ*sbcB*::*Tm*^{R}, *comEA-mCherry*, *P*$_{tac}$-*tfoX*, Δ*luxO*, *lacZ*::*lacI*^{q}, *pilA*^{S67C}, Δ*VC1807*::*Cm*^{R}	Fig. 2	Δ*sbcB* for ComEA-mCherry localization assays
SAD1063	*Kan*^{R}-*Ptac-tfoX*, Δ*mutS*	Fig. 3B-C	parent for *in vivo* branch migration assays
TND2585 / SAD3582	Δ*sbcB*::*Spec*^{R}, *Kan*^{R}-*Ptac-tfoX*, Δ*mutS*	Fig. 3B-C	Δ*sbcB* for *in vivo* branch migration assays
SAD1071	Δ*comM*::*Spec*^{R}, *Kan*^{R}-*Ptac-tfoX*, Δ*mutS*	Fig. 3B-C	Δ*comM* for *in vivo* branch migration assays
TND1474 / SAD3583	Δ*lacZ*::*P*$_{lac}$-*CFP-parB*$_{P1}$-*mCherry-parB*$_{MT1}$ *Zeo*^{R}, *0.11Mbp*::*parS*$_{MT1}$, *GFP-comM*, *P*$_{tac}$-*tfoX*, Δ*luxO*, *pilA*^{S67C}, Δ*VC1807*::*Cm*^{R}	Fig. 4A-C	parent for GFP-ComM localization assays
TND1509 / SAD3584	Δ*sbcB*::*Tm*^{R}, Δ*lacZ*::*P*$_{lac}$-*CFP-parB*$_{P1}$-*mCherry-parB*$_{MT1}$ *Zeo*^{R}, *0.11Mbp*::*parS*$_{MT1}$, *GFP-comM*, *P*$_{tac}$-*tfoX*, Δ*luxO*, *pilA*^{S67C}, Δ*VC1807*::*Cm*^{R}	Fig. 4B-C	Δ*sbcB* for GFP-ComM localization assays
SAD3547	*E. coli* TG1, pKT25-*sbcB*^{D13A,E15A}	Fig. 7	Harbors theT25-SbcB* vector for BACTH analysis
SAD3549	*E. coli* TG1, pKNT25-*sbcB*^{D13A,E15A}	Fig. 7	Harbors the SbcB*-T25 vector for BACTH analysis
SAD3558	*E. coli* TG1, pUT18C-*sbcB*^{D13A,E15A}	Fig. 7	Harbors the T18-SbcB* vector for BACTH analysis
SAD3551	*E. coli* TG1, pUT18-*sbcB*^{D13A,E15A}	Fig. 7	Harbors the SbcB*-T18 vector for BACTH analysis
TMN0416 / SAD3585	*E. coli* TG1, pUT18C-*recA*	Fig. 7	Harbors the T18-RecA vector for BACTH analysis
TMN0419 / SAD3587	*E. coli* TG1, pUT18-*recA*	Fig. 7	Harbors the RecA-T18 vector for BACTH analysis
TMN0417 / SAD3586	*E. coli* TG1, pUT18C-*dprA*	Fig. 7	Harbors the T18-DprA vector for BACTH analysis
TMN0420 / SAD3588	*E. coli* TG1, pUT18-*dprA*	Fig. 7	Harbors the DprA-T18 vector for BACTH analysis
SAD2240	*E. coli* TG1, pUT18C	Fig. 7	Harbors the T18 empty vector for BACTH analysis
SAD2241	*E. coli* TG1, pUT18C-zip	Fig. 7	Harbors the T18-zip vector for BACTH analysis
SAD2238	*E. coli* TG1, pKT25-zip	Fig. 7	Harbors the T25-zip vector for BACTH analysis

*Multiple Strain# designations indicate that the strain was stocked in two independent strain collections.

663 **Table S2** – *Primers used in this study*
664

Primer*	Sequence (5' → 3')	Description
BBC688	TGGATGAGTGCTAAATGATGC	Δ*sbcB* (*i.e.*, ΔVC1234) F1
BBC689	gtcgacggatccccggaatCATGTGGCTTACCAAATCGC	Δ*sbcB* (*i.e.*, ΔVC1234) R1
BBC690	gaagcagctccagcctacaTGCTAACATCGTTTATTTTTACTTGC	Δ*sbcB* (*i.e.*, ΔVC1234) F2
BBC691	AACATGGTAAACAGCACCATC	Δ*sbcB* (*i.e.*, ΔVC1234) R2
DOG0582	ACATCTGGCAGATCTGATTTCAC	Δ*pilQ* (*i.e.*, ΔV2630) F1
DOG0583	gtcgacggatccccggaatCAACCGATTATTTTAAAGCCAGCTTG	Δ*pilQ* (*i.e.*, ΔV2630) R1
DOG0584	gaagcagctccagcctacaTAACTTAGCGTGTGCGTAACAAG	Δ*pilQ* (*i.e.*, ΔV2630) F2
DOG0585	TTGTGTTTGCTCTAACGTTTGC	Δ*pilQ* (*i.e.*, ΔV2630) R2
BBC411	CAAGATTGGCAATGGAGCGAC	Δ*comEC* (*i.e.*, ΔVC1879) F1
BBC412	gtcgacggatccccggaatCATAATCCCGTATGCCAAGAAAATTC	Δ*comEC* (*i.e.*, ΔVC1879) R1
BBC546	gaagcagctccagcctacaATGACCGATACTCAGTCTAACC	Δ*comEC* (*i.e.*, ΔVC1879) F2
BBC414	TCATCCATGCTCATGCTGCG	Δ*comEC* (*i.e.*, ΔVC1879) R2
ABD820	CGCTCTTATCTGCTTGGATAATGG	Δ*dprA* (*i.e.*, ΔVC0048) F1
ABD998	gtcgacggatccccggaatCATTAACTGGCATCATCAACC	Δ*dprA* (*i.e.*, ΔVC0048) R1
ABD999	gaagcagctccagcctacaTAGCTATGATGATGGATATTTTGATG	Δ*dprA* (*i.e.*, ΔVC0048) F2
ABD996	GGTTTGGTTATCCGGATCACAC	Δ*dprA* (*i.e.*, ΔVC0048) R2
ABD855	CATGAATCACTTTGGCATGAGG	Δ*comM* (*i.e.*, ΔVC0032) F1
ABD856	gtcgacggatccccggaatCATTGCTTCCCTTAGTATTTGATC	Δ*comM* (*i.e.*, ΔVC0032) R2
ABD857	gaagcagctccagcctacaTAGTACTCTGACCTGCAGAGTTC	Δ*comM* (*i.e.*, ΔVC0032) F2
ABD858	AAATTCCAGAAAAACCACGTC	Δ*comM* (*i.e.*, ΔVC0032) R2
BBC678	TGGATGCCAATCAACATTCG	Δ*recJ* (*i.e.*, ΔVC2417) F1
BBC679	gtcgacggatccccggaatCATACTGTGACAGGCCAAAG	Δ*recJ* (*i.e.*, ΔVC2417) R1
BBC680	gaagcagctccagcctacaGAAGCGAAATGATTGAAAACAACG	Δ*recJ* (*i.e.*, ΔVC2417) F2
BBC681	GATCGCATCCACAATGTTAGC	Δ*recJ* (*i.e.*, ΔVC2417) R2
DOG0185	TTCACTTCACCCAGTACACGC	Δ*exoVII* (*i.e.*, ΔVC0766) F1
DOG0186	gtcgacggatccccggaatCAACGCTGATTCCTCAGACG	Δ*exoVII* (*i.e.*, ΔVC0766) R1
DOG0187	gaagcagctccagcctacaTTAATGGATGGTGAGATTCTCTC	Δ*exoVII* (*i.e.*, ΔVC0766) F2
DOG0188	AGTTTGTAGAGGTTGTTATGGTAC	Δ*exoVII* (*i.e.*, ΔVC0766) R2
DOG0190	AGAAGAACTCTGTTTTGCATTAGAAC	Δ*exoIX* (*i.e.*, ΔVC0898) F1
DOG0191	gtcgacggatccccggaatCAAGCGACGAGTTCATGCTTG	Δ*exoIX* (*i.e.*, ΔVC0898) R1
DOG0192	gaagcagctccagcctacaTAAATCCCCTCTGATTAGCATC	Δ*exoIX* (*i.e.*, ΔVC0898) F2
DOG0193	TTAACCCTGACGTGACCGTG	Δ*exoIX* (*i.e.*, ΔVC0898) R2
BBC5040	CAAGTagCGTAcgCGAAAAAGAAGAATGTGGGCTGGTGTTCTTGCT	*sbcB*^{D13AE15A} R1
BBC5041	TTCTTTTTCGcgTACGctACTTGGGGAGTCAATCCCGCAAAAGATC	*sbcB*^{D13AE15A} F2

BBC4977	gcctggagtgcctaatgagGCTGAACAAATAATGGGATAGC	Amplify *sbcB* to clone at an ectopic locus with its native promoter intact F
BBC3101	tgtaggctggagctgcttcTTAGCAAGCGAGTTTTTCCACG	Amplify *sbcB* to clone at an ectopic locus with its native or P_{tac} promoter intact R
BBC5065	tttagcgatttggtaagccacATGATGAATGACGGTAAGCAAC	Amplify *E. coli* sbcB to clone at an ectopic locus F
BBC5066	tgtaggctggagctgcttcTTAGACAATCTCTTCCGCGTAC	Amplify *E. coli* sbcB to clone at an ectopic locus R
BBC3100	caatttcacacaggatcccgggaggaggtAGCCACATGCAGCAAGAACAC	Amplify *sbcB* to clone at an ectopic locus under the control of P_{tac} F
BBC5203	gcctggagtgcctaatgagTTCAAGGTTGGCTCAAAGTGG	Amplify *recA* to clone at an ectopic locus with its native promoter intact F
BBC655	tgtaggctggagctgcttcTTAAAACTCTTCTGGCACCGC	Amplify *recA* to clone at an ectopic locus with its native promoter intact R
BBC5145	AGGTagCGTAcgCGTGAAACAAAAAGGTAGATTGTTGCTTACCGTC	*E. coli sbcB*^{D15AE17A} R1
BBC5146	TTGTTTCACGcgTACGctACCTTTGGCACGCACCCCGCGTTAGATC	*E. coli sbcB*^{D15AE17A} F2
BBC5195	gcaggtggagcaggtggaCAGCAAGAACACCAGCCCAC	Amplify *sbcB** for TXX-*sbcB** or *sbcB**-TXX for BACTH F
BBC3103	tgtaggctggagctgcttcTTAGGCTGCGATTAATAGCTCTTTAG	Amplify *sbcB** for TXX-*sbcB** for BACTH R
BBC5196	tccaccacttccacctgcGCAAGCGAGTTTTTCCACGTAATGG	Amplify *sbcB** for *sbcB**-TXX for BACTH R
TMN0198	gcaggtggagcaggtggaGACGAGAATAAACAGAAGGCAC	Amplify *recA* for TXX-*recA* or *recA*-TXX for BACTH F
TMN0199	tgtaggctggagctgcttcTTAAAACTCTTCTGGCACCGC	Amplify *recA* for TXX-*recA* for BACTH R
TMN0200	tccaccacttccacctgcAAACTCTTCTGGCACCGC	Amplify *recA* for *recA*-TXX for BACTH R
TMN0210	gcaggtggagcaggtggaAAAGATCAGGATTTAGCGGCATG	Amplify *dprA* for TXX-*dprA* or *dprA*-TXX for BACTH F
TMN0211	tgtaggctggagctgcttcCTAGCCTCTCCCCTTTCTAATATAGC	Amplify *dprA* for TXX-*dprA* for BACTH R
TMN0212	tccaccacttccacctgcGCCTCTCCCCTTTCTAATATAGCC	Amplify *dprA* for *dprA*-TXX for BACTH R
PP327	IR800CW-AAATTTGGCTATTGATAGTGCTCATTG	IR800 ssDNA oligo used for ssDNA exonuclease activity assays

*Lower case nucleotides on the 5' end demarcate overlap sequences for SOE PCR. While internal lower case nucleotides demarcate point mutations.